Mössbauer spectral study of the magnetocaloric FeMnP1-xAsx compounds

Hermann, R.P.; Tegus, O.; Bruck, E.H.; Buschow, K.H.J.; de Boer, F.R.; Long, G.J.; Grandjean, F.

Published in:
Physical Review B

Mössbauer spectral study of the magnetocaloric $FeMnP_{1-x}As_x$ compounds

Raphaël P. Hermann,[1] O. Tegus,[2] E. Brück,[2] K. H. J. Buschow,[2] F. R. de Boer,[2] Gary J. Long,[3] and Fernande Grandjean[1]
[1]*Département de Physique, B5, Université de Liège, B-4000 Sart-Tilman, Belgium*
[2]*Van der Waals-Zeeman Instituut, Universiteit van Amsterdam, Valkenierstraat 65, 1018 XE Amsterdam, The Netherlands*
[3]*Department of Chemistry, University of Missouri-Rolla, Rolla, Missouri 65409-0010, USA*
(Received 14 May 2004; published 23 December 2004)

The magnetic phase transitions in the $FeMnP_{1-x}As_x$ compounds with x= 0.25, 0.35, 0.45, 0.50, and 0.55, have been studied by iron-57 Mössbauer spectroscopy. The ferromagnetic and antiferromagnetic spectra have been analyzed with a model that takes into account the random distribution of the P and As near-neighbor anions of a given iron site. This distribution is a binomial distribution of the contributions to the spectra of each iron with n As near neighbors. A magnetostriction model has been used to characterize the temperature induced paramagnetic to ferromagnetic first-order phase transition and order parameters, η_F=2.6, 2.3, 2.0, 1.57, and 1.43 have been obtained for x=0.25, 0.35, 0.45, 0.50, and 0.55, respectively. A detailed phase diagram has been derived from the Mössbauer spectral analysis and reveals a magnetic triple point at x= ~0.35 and ~210 K. A model that takes into account the random binomial P and As distribution and the contribution from the iron and manganese magnetic sublattices yields excellent fits of the spectral components assigned to the ferromagnetic and incommensurate antiferromagnetic components for the x=0.25 and 0.35 compounds at all temperatures.

DOI: 10.1103/PhysRevB.70.214425 PACS number(s): 75.30.Sg, 76.80.+y, 75.50.Ee, 75.50.Bb

I. INTRODUCTION

Materials in which a magnetic phase transition is accompanied by a structural transition[1,2] or by magnetostriction[3] are promising for room temperature magnetic refrigeration.[4] In such materials the magnetic phase transitions are first-order and a large change in entropy occurs upon magnetic ordering. A refrigerating heat pump cycle can be devised through the alternative application and removal of an external magnetic field on a magnetocaloric material.[5–8] First, the increase in thermal energy that results from the alignment of the magnetic moments when an external magnetic field is applied is dissipated by thermal transfer to a heat sink, i.e., to the hot point. Second, thermal energy is removed from the heat source, i.e., the cold point, when the external magnetic field is removed because of the resulting randomization of the magnetic moments, a randomization that cools the magnetocaloric material. The resulting magnetocaloric cooling power increases with an increase in both the magnetic moment of the compound and the applied magnetic field.[8,9] Hence, materials containing a rare-earth with a large magnetic moment are of particular interest.[1,10]

Recently the $FeMnP_{1-x}As_x$ compounds have been shown[3,11] to be good candidates for magnetocaloric cooling applications near room temperature. These compounds have the advantage of both a tailorable Curie temperature as a function of x, and inexpensive constituents as compared with many rare-earth containing materials. Herein, the $FeMnP_{1-x}As_x$ compounds have been studied in detail by iron-57 Mössbauer spectroscopy. The observed first-order ferromagnetic to paramagnetic phase transition is described with a magnetostriction model. The Mössbauer spectra of $FeMnP_{0.75}As_{0.25}$ and $FeMnP_{0.65}As_{0.35}$ in their incommensurate magnetic phase are fit with a model that takes into account the oscillating iron magnetic moments, the helical arrangement of the manganese magnetic moments, and the binomial distribution of P and As near neighbor, the same distribution as was used for the compounds with higher As content. Finally, an improved magnetic phase diagram for the $FeMnP_{1-x}As_x$ compounds is established.

II. EXPERIMENT

The samples studied herein are the same as those prepared and described earlier.[3] The iron-57 Mössbauer spectra were recorded between 4.2 and 320 K on a constant acceleration spectrometer which utilized a rhodium matrix cobalt-57 source and was calibrated at 295 K with α-iron powder. The isomer shifts reported herein are given relative to α-iron at 295 K. The sample temperature in the Janis SV-300 cryostat was controlled with a LakeShore 330 temperature controller and a silicon diode mounted on the copper sample holder. The accuracy of the sample temperature is better than ±0.5 K. The thickness of the absorbers was 28, 15, 30, 28, and 35 mg/cm^2 of $FeMnP_{1-x}As_x$ for x=0.25, 0.35, 0.45, 0.50, and 0.55, respectively.

III. STRUCTURE AND DISTRIBUTION OF PHOSPHORUS AND ARSENIC

In the $FeMnP_{1-x}As_x$ compounds which crystallize with the Fe_2P hexagonal structure in the $P\bar{6}2m$ space group, phosphorus and arsenic are randomly distributed on the 1b and 2c sites, whereas iron occupies the tetrahedral 3f site and manganese occupies the pyramidal 3g site.[12,13] Although the 3f and 3g sites are fully occupied, some iron-manganese disorder on these sites has been reported[13,14] and is also detected herein in the paramagnetic Mössbauer spectra of some of the compounds. Because phosphorus and arsenic are randomly distributed in the tetrahedral coordination environment of the iron, five different iron near-neighbor environments are possible and, hence, the magnetic contributions to the Mössbauer spectra have been fit with a binomial distribution

model. Thus, the relative iron-57 spectral absorption areas of the contributions with n arsenic neighbors are given by the probabilities

$$P(n) = C_4^n x^n (1-x)^{4-n}. \quad (1)$$

The isomer shift, quadrupole shift, and hyperfine field for n arsenic near neighbors are given by the linear relationships,

$$\delta(n) = \delta(0) + n\Delta\delta, \quad (2a)$$

$$\epsilon(n) = \epsilon(0) + n\Delta\epsilon, \quad (2b)$$

and

$$H(n) = H(0)(1 - n\Delta H), \quad (2c)$$

where $\delta(0)$, $\epsilon(0)$, and $H(0)$ are the isomer shift, quadrupole shift, and hyperfine field observed for zero arsenic near neighbors, $\Delta\delta$ and $\delta\epsilon$ are the incremental isomer shift and quadrupole shift resulting from one additional arsenic near neighbor, and ΔH is the *percentage reduction* in the hyperfine field resulting from one additional arsenic near neighbor. This percentage reduction description was chosen because preliminary fits indicated that the absolute reduction in the field is not constant as a function of temperature, whereas the percentage reduction is essentially constant, except at temperatures near the first-order magnetic phase transition. The effect of the substitution of a near-neighbor anion on the hyperfine fields has been studied[15,16] in the isostructural $Fe_2P_{1-x}B_x$ and $Fe_2P_{1-x}Si_x$ compounds and, more specifically, the substitution of P by As in $FeMnP_{1-x}As_x$ is known[14] to reduce the hyperfine field by about 1.4 T per substituted anion.

By using the probabilities in Eq. (1), the average values for the hyperfine parameters given in Eq. (2) are given by

$$\langle\delta\rangle = \delta(0) + 4x\Delta\delta, \quad (3a)$$

$$\langle\epsilon\rangle = \epsilon(0) + 4x\Delta\epsilon, \quad (3b)$$

and

$$\langle H\rangle = H(0)(1 - 4x\Delta H). \quad (3c)$$

IV. MÖSSBAUER SPECTRAL RESULTS

The Mössbauer spectra of $FeMnP_{1-x}As_x$ with $x=0.25$, 0.35, 0.45, 0.50, and 0.55, measured at 4.2 K, are shown in Fig. 1. The 4.2 K spectra for $x \geqslant 0.35$ exhibit similar sextets that may be associated with a ferromagnetic phase that gives broad outer and narrow inner spectral lines, as is expected for a hyperfine field distribution resulting from a different number of arsenic near neighbors. In contrast, the 4.2 K spectrum of $FeMnP_{0.75}As_{0.25}$ exhibits a more complex shape that results from the superposition of a minor contribution of ca. 20% that is similar to the spectra obtained for $x \geqslant 0.35$ and a major contributon with a smaller hyperfine field that is associated with an antiferromagnetic phase.[14]

The Mössbauer spectra measured around the first-order ferromagnetic phase transition for $x=0.55$, 0.50, 0.45, and 0.35 are shown in Fig. 2. These spectra were measured with

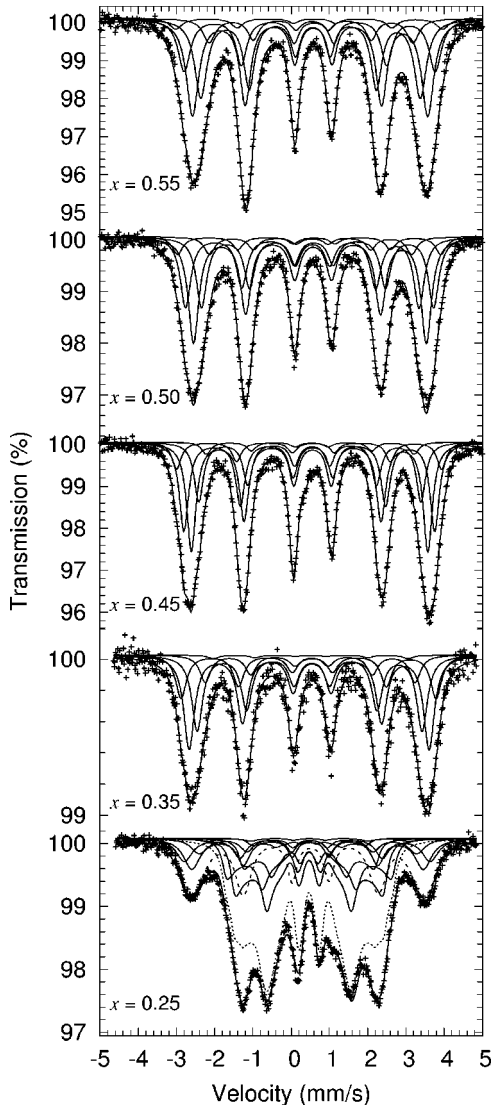

FIG. 1. The Mössbauer spectra of $FeMnP_{1-x}As_x$ obtained at 4.2 K. For $x=0.25$ the dashed and the dotted lines are the sum of the binomial ferromagnetic and antiferromagnetic components, respectively.

increasing temperature starting at 4.2 K. The likely presence of a small thermal hysteresis was not investigated. The coexistence of the paramagnetic and ferromagnetic phases over a temperature range of as much as 10 K is clearly revealed in these spectra. Further, the hyperfine field of the ferromagnetic phase remains a substantial fraction of the field observed at 4.2 K, even in spectra in which ca. 80% of the compound is paramagnetic. The Mössbauer spectra of $FeMnP_{0.75}As_{0.25}$, measured between 210 and 90 K, are shown in Fig. 3. They reveal that the relative area of the broad outer sextet, a sextet that is similar to the sextet observed for the other compositions, decreases as the temperature increases from 4.2 to 190 K. In contrast to the spectra for $x \geqslant 0.35$, the hyperfine field, characteristic of the antiferromagnetic phase, is substantially smaller near the Néel temperature than at 4.2 K.

The ferromagnetic contributions to the spectra of the compounds with $x \geqslant 0.35$ were fit with the binomial distribution

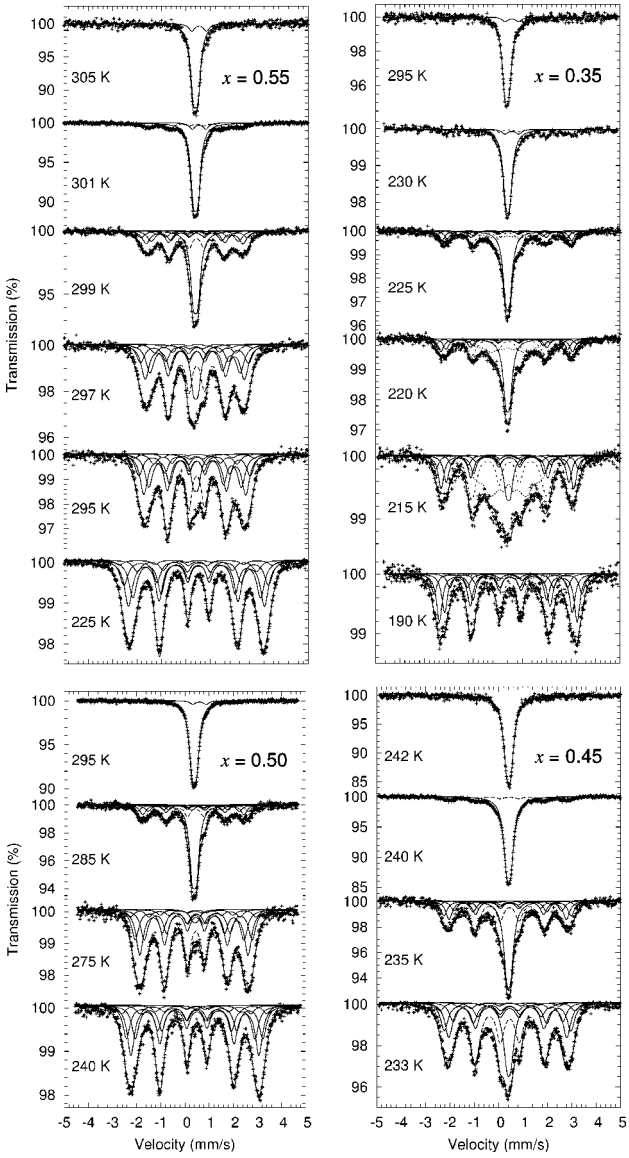

FIG. 2. The Mössbauer spectra of $FeMnP_{1-x}As_x$, where $x = 0.35$, 0.45, 0.50, and 0.55, going clockwise from $x = 0.35$ in the upper right-hand side panel. The dashed line is the sum of the ferromagnetic components. For $x = 0.35$, the dotted line is the sum of the antiferromagnetic components. The small doublet in the paramagnetic spectra, for $x = 0.35$, 0.50, and 0.55, corresponds to iron on the pyramidal manganese site.

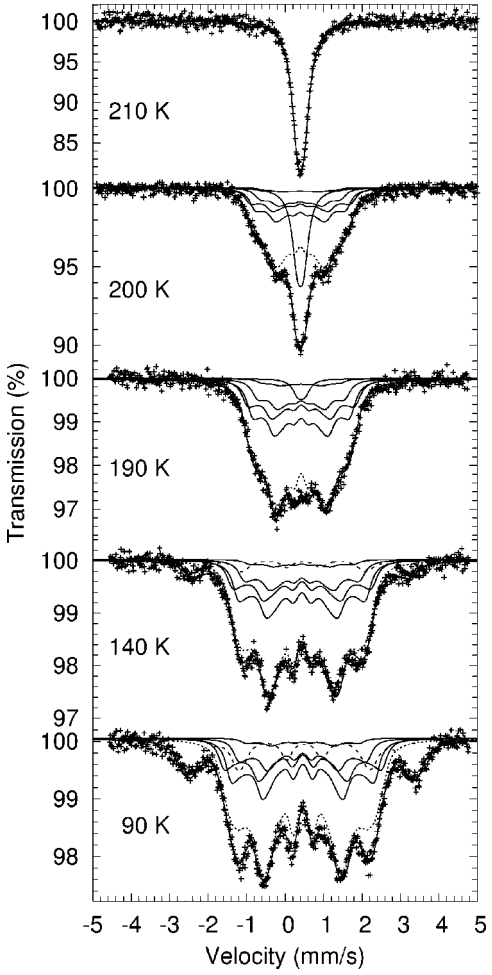

FIG. 3. The Mössbauer spectra of $FeMnP_{0.75}As_{0.25}$ obtained at the indicated temperatures. The dashed and dotted lines are the sum of the ferromagnetic and antiferromagnetic components, respectively. The weakest antiferromagnetic component assigned to the iron with four arsenic near neighbors is not shown.

model described by Eqs. (1) and (2). For each composition, x, the values of $\Delta\delta$, $\epsilon(0)$, and $\Delta\epsilon$ were first fit for each spectrum as a function of temperature, and subsequently constrained to their thermal average, because the preliminary fits indicated essentially temperature independent values for these hyperfine parameters. Hence, in the final fits, the baseline, the spectral absorption area, the isomer shift, $\delta(0)$, the hyperfine field, $H(0)$, the percentage hyperfine field reduction, ΔH, and the linewidth, Γ, were adjusted. The paramagnetic contribution to the spectra, p, was fit with one symmetric doublet with an isomer shift, δ, constrained to the $\langle\delta\rangle$ value obtained from Eq. (3a), for the spectra in which the ferromagnetic phase is present. For each composition, x, the quadrupole splitting, ΔE_Q, of the doublet was first fit as a free parameter and subsequently constrained to its virtually temperature independent value. The spectral parameters resulting from these spectral fits are given in Tables I and II. In these tables, and all subsequent tables, the error relative to a reported value is approximately two on the last reported digit.

For the Mössbauer spectra of $FeMnP_{0.75}As_{0.25}$, the minor component, of spectral area f, with the large field has been fit with the model described for the compounds with $x \geqslant 0.35$. This component can be attributed to a ferromagnetic phase similar to that observed in $FeMnP_{1-x}As_x$, with $x \geqslant 0.35$.[14] Several models were tried to fit the major component with the small field, a component that can be attributed to the antiferromagnetic $FeMnP_{1-x}As_x$ phase.[14] First, a second binomial distribution with smaller fields was included in the fits. These fits were satisfactory only at 4.2 and 90 K, indicating that the antiferromagnetic contribution cannot be fit with the simple binomial distribution of magnetic sextets used for the compounds with $x \geqslant 0.35$ and that the model must be amended.

TABLE I. The Mössbauer spectral hyperfine parameters for $FeMnP_{1-x}As_x$.

x	T, K	$\langle\delta\rangle$, mm/s	H (0), T	ΔH, %	$\langle H\rangle$, T	Γ, mm/s	p, %	Constraints, mm/s
0.55	307	0.389				0.30	100	$\Delta\delta=-0.002$
	305	0.397				0.30	100	$\epsilon(0)=-0.14$
	301	0.401	14.5	8.5	11.8	0.29	80	$\Delta\epsilon=0.027$
	299	0.400	14.8	8.4	12.1	0.30	39	$\langle\epsilon\rangle=-0.08$
	297	0.407	14.9	7.6	12.4	0.31	14	$\Delta E_Q=0.18$
	295	0.410	15.3	7.7	12.7	0.29	9	
	225	0.477	19.4	5.5	17.1	0.31	0	
	155	0.510	20.5	5.5	18.1	0.31	0	
	90	0.528	21.1	5.7	18.5	0.30	0	
	85	0.535	21.2	5.7	18.6	0.32	0	
	50	0.538	21.5	5.8	18.7	0.31	0	
	4.2	0.539	21.7	5.9	18.9	0.30	0	
0.50	295	0.394				0.30	100	$\Delta\delta=-0.002$
	285	0.401	15.5	8.1	13.0	0.28	51	$\epsilon(0)=-0.13$
	275	0.419	16.2	6.9	13.9	0.32	3	$\Delta\epsilon=0.023$
	240	0.460	18.6	5.8	16.5	0.32	0	$\langle\epsilon\rangle=-0.08$
	190	0.478	19.6	5.8	17.3	0.32	0	$\Delta E_Q=0.18$
	140	0.502	20.2	5.5	17.9	0.34	0	
	90	0.523	20.8	5.8	18.4	0.33	0	
	4.2	0.533	21.5	6.0	18.9	0.31	0	
0.45	295	0.381				0.29	100	$\Delta\delta=-0.002$
	265	0.405				0.31	100	$\epsilon(0)=-0.12$
	240	0.418	17.3	7.3	15.0	0.31	82	$\Delta\epsilon=0.02$
	235	0.416	17.4	7.2	15.2	0.32	36	$\langle\epsilon\rangle=-0.08$
	233	0.419	17.2	6.3	15.3	0.37	19	$\Delta E_Q=0.16$
	190	0.459	18.9	5.3	17.1	0.30	0	
	140	0.486	20.0	5.4	18.1	0.29	0	
	90	0.506	20.8	5.4	18.8	0.29	0	
	4.2	0.521	21.5	5.3	19.5	0.29	0	

Second, because the antiferromagnetic structure is incommensurate,[13,14] a fit with the expected field distribution[17] for a simplified one dimensional incommensurate structure was attempted. If the magnetic and crystalline structures are incommensurate, the Mössbauer nuclei corresponding to the magnetic ions must be considered as uniformly distributed in the unit cell of the magnetic lattice, with lattice constant a_M. The hyperfine field experienced by a nucleus at the position x_M, is given by

$$H_{\mathrm{AF}} = C\mu \sin\theta, \tag{4}$$

where C is a proportionality constant, μ is the magnetic moment, and $\theta=2\pi x_M/a_M$. The sign of the hyperfine field is not observed in the Mössbauer spectrum in the absence of an applied field and by symmetry, the incommensurate magnetic spectral component is then obtained by integration over $0 \leqslant \theta \leqslant \pi/2$, of the magnetic sextets with the hyperfine fields as given by Eq. (4). The integration was performed for each term of the binomial arsenic and phosphorus distribution by summing 41 sextets corresponding to θ values regularly spaced in the interval $0 \leqslant \theta \leqslant \pi/2$. Unfortunately, no satisfactory fits were obtained unless an unphysically large number of odd harmonic terms, $\mu_{2n+1}\sin[(2n+1)\theta]$, with $n>1$, were added to the description in Eq. (4).[17]

Finally, because there are two noncollinear magnetic iron and manganese sublattices in the compounds under study,[13] a modified description of the incommensurate structure was adopted. The hyperfine field was described as

$$H_{\mathrm{AF}} = C_1\mu_{\mathrm{Fe}} + C_2\mu_{\mathrm{Mn}} \sin\theta, \tag{5}$$

where C_1 and C_2 are proportionality constants for the two sublattices, and μ_{Fe} and μ_{Mn} are the moments for the iron and manganese magnetic sublattices, respectively. The relationship of this description with the crystalline structure will be discussed in detail below. A fitting model that takes into account both the incommensurate magnetic structure, as described in Eq. (5), and the binomial distribution of the phosphorus and arsenic near neighbors was used and gave excel-

TABLE II. The Mössbauer spectral hyperfine parameters for $FeMnP_{0.65}As_{0.35}$.

T, K	$\langle\delta\rangle$, mm/s	H (0), T	ΔH, %	$\langle H\rangle$, T	$\langle H_{AF}\rangle$, T	Γ, mm/s	p, %	a, %	f, %	Constraints, mm/s
295	0.371					0.30	100	0	0	$\Delta\delta=-0.002$
230	0.404	16.9	6.1	15.5		0.30	77	0	23	$\epsilon(0)=-0.10$
225	0.399	17.8	7.0	15.9	6	0.28	44	16	40	$\Delta\epsilon=0.022$
220	0.401	17.9	7.1	16.2	6.7	0.28	31	26	43	$\langle\epsilon\rangle=-0.07$
215	0.430	18.1	6.8	16.3	6.9	0.28	9	39	52	$\Delta E_Q=0.16$
190	0.462	18.7	6.8	17.0	7	0.28	0	7	93	
140	0.475	19.4	6.1	17.7		0.30	0	0	100	
90	0.502	20.1	6.1	18.4		0.30	0	0	100	
4.2	0.510	20.9	6.4	19.0		0.31	0	0	100	

lent, physically reasonable, fits at all temperatures. The same percentage hyperfine field reduction defined in Eq. (2c) was used for the antiferromagnetic hyperfine field reduction, ΔH_{AF}. It should be noted that the fits were obtained through a classical minimization of χ^2 as a function of the hyperfine parameters and not with a hyperfine field distribution routine.[14] In these fits, the percentage decremental hyperfine field for the ferromagnetic phase was constrained to 5.8% in order to reduce the number of free parameters. The resulting spectral parameters for $FeMnP_{0.75}As_{0.25}$ are given in Table III. The average value of the hyperfine field, $\langle H_{AF}\rangle=(C_1\mu_{Fe}+2C_2\mu_{Mn}/\pi)(1-4x\Delta H_{AF})$, is obtained by averaging over $0\leqslant\theta\leqslant\pi/2$.

The fitting approach used for $x=0.25$ was also applied to fit the antiferromagnetic component that is observed in the region $180<T<230$ K in the spectra of $FeMnP_{0.65}As_{0.35}$. Because the percentage decremental field could not otherwise be reliably determined, its value for the antiferromagnetic phase, with spectral area a, was constrained to 10%, as was observed for $FeMnP_{0.75}As_{0.25}$ at 200 K.

The temperature dependence of the average isomer shift, $\langle\delta\rangle$, is in good agreement with the Debye model for the second order Doppler shift[18] and a Debye temperature of 420 ± 20 K was obtained from a simultaneous fit of $\langle\delta\rangle$ as a function of temperature for all the $FeMnP_xAs_{1-x}$ compounds, below 170 K. The asymptotic isomer shifts, $\langle\delta\rangle^0$, obtained from this fit are 0.657, 0.648, 0.633, 0.624, and 0.588 ± 0.005 mm/s for $x=0.55$, 0.50, 0.45, 0.35, and 0.25, respectively. At temperatures above 170 K, the isomer shifts decrease more than would be expected from the Debye model, probably because of the influence[19] of the magnetostriction accompanying the ordering upon the isomer shift. Further, the increase of $\langle\delta\rangle^0$ in x results from the large increase in the a lattice parameter with increasing x.[13,20,21]

The average quadrupole shift in the ferromagnetic phase is temperature independent and identical to the previously reported[14] value of -0.08 mm/s for all compounds. In the paramagnetic phase a temperature independent quadrupole splitting, ΔE_Q, of 0.16 and 0.18 mm/s is observed for the compounds with $x<0.45$ and $x\geqslant0.45$, respectively, in good agreement with the 0.16 mm/s value reported earlier.[14] This indicates both that the principal axis of the electric field gradient tensor lies in the basal ab plane[14] and that the quadrupole splitting is positive. In the antiferromagnetic phase, the quadrupole shift has been constrained to be zero.

In the paramagnetic spectra of $FeMnP_{1-x}As_x$ with $x=0.55$, 0.50, and 0.35, a small doublet with ca. 5% relative area and an isomer shift, $\delta=0.54$, 0.61, and 0.58 mm/s for $x=0.55$ at 305 K, $x=0.50$ at 295 K, and for $x=0.35$ at 295 K, respectively, and an identical quadrupole splitting, ΔE_Q, of 0.55 mm/s, is observed for all three compounds. The presence of this additional spectral component was previously reported and related to iron on the pyramidal manganese site.[13,14,22] Interestingly, $FeMnP_{0.55}As_{0.45}$ does not exhibit this additional component. It is likely that the slight iron-manganese disorder that gives rise to this spectral component is dependent on the preparation. Further, it cannot be

TABLE III. The Mössbauer spectral hyperfine parameters for $FeMnP_{0.75}As_{0.25}$.

T, K	$\langle\delta\rangle$, mm/s	$\langle H_{Ferro}\rangle$, T	$C_1\mu_{Fe}$, T	$C_2\mu_{Mn}$, T	ΔH_{AF}, %	$\langle H_{AF}\rangle$, T	Γ, mm/s	p, %	a, %	f, %
295	0.358						0.30	100	0	0
210	0.403						0.37	100	0	0
200	0.398		2.8	5.6	10	5.7	0.32	24	76	0
190	0.420		3.0	5.9	9	6.2	0.32	4	96	0
140	0.441	16.8	4.2	7.3	8	8.1	0.32	0	90	10
90	0.464	17.7	5.8	7.2	9	9.4	0.30	0	77	23
4.2	0.468	18.4	7.3	6.4	10	10.2	0.25	0	67	33

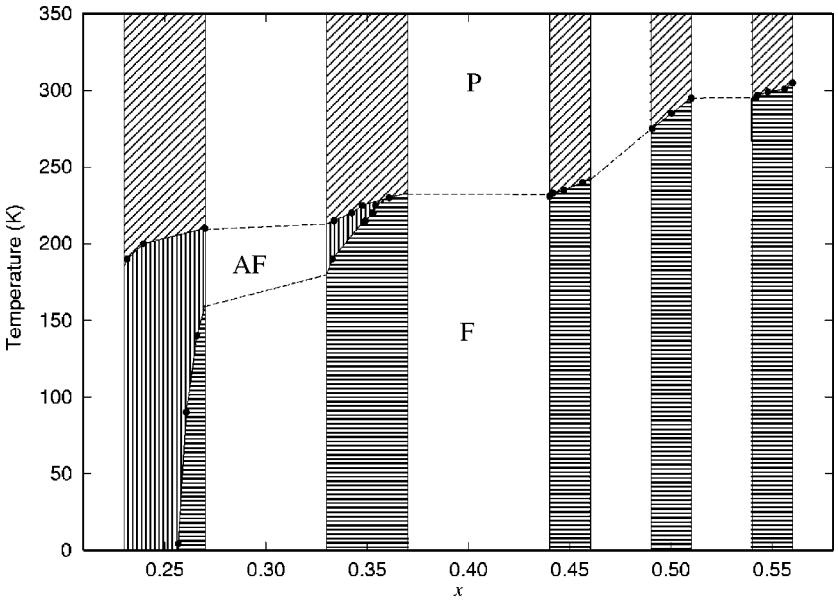

FIG. 4. The phase diagram of $FeMnP_{1-x}As_x$ obtained from the Mössbauer spectral results. The diagonal hatching denotes the paramagnetic phase, P, the horizontal hatching the ferromagnetic phase, F, and the vertical hatching the antiferromagnetic phase, AF. In the construction of this phase diagram, a compositional range of ~0.01 is assumed for $x=0.55$, 0.50, and 0.45. This range has been doubled to facilitate the reading of the diagram for $x=0.25$ and 0.35. Within the ranges corresponding to each compound, the relative width of each phase corresponds, at a given temperature, to the percentage of this phase observed in the Mössbauer spectra. The measured data, black dots, are interpolated and extrapolated to generate the phase boundaries.

ruled out that the disorder does not significantly affect the Curie temperature of the compounds, however, a systematic study of this effect is difficult. In the fits of the magnetic phases the contribution from the iron on the manganese site is too weak to be resolved and has been neglected.

V. THE ORDER OF THE PHASE TRANSITIONS

The spectral parameters corresponding to the percentage of ferromagnetic, antiferromagnetic, and paramagnetic phases as a function of x and T permit the construction of a magnetic phase diagram for $FeMnP_{1-x}As_x$, see Fig. 4. This phase diagram closely resembles the phase diagram obtained from neutron scattering measurements,[13,20] and the most important difference is in the higher ferromagnetic to paramagnetic transition temperature observed for $x=0.50$ and 0.55. In addition, the Mössbauer spectra obtained for $x=0.25$ and 0.35 clearly reveal a magnetic triple point[13,20] at ca. $x=0.35$ and 210 K. Further the Mössbauer spectra reveal that the antiferromagnetic to ferromagnetic low temperature phase boundary is at approximately $x=0.25$. Even though this phase diagram is certainly qualitatively correct, a quantitative interpretation should be avoided because different preparation methods for the $FeMnP_{1-x}As_x$ compounds may lead to more or less homogeneous materials and to a somewhat different magnetic phase diagram.

A coexistence of the ferromagnetic and paramagnetic phases is observed for the first-order magnetic transition in $FeMnP_{1-x}As_x$, where $x=0.35$, 0.45, 0.50, and 0.55. The relative increase in the amount of paramagnetic phase may be described with a simple phenomenological model that supposes that the distribution of the Curie temperature in different sample grains is Gaussian and, hence,

$$p(T)=\frac{1}{\sqrt{2\pi}}\int_{-\infty}^{(T-T_C)/w} e^{-z^2/2}\,dz=\frac{1}{2}+\frac{1}{2}\mathrm{erf}[(T-T_C)/(\sqrt{2}w)], \tag{6}$$

where p is the paramagnetic fraction and w is the width of the Gaussian distribution, and thus the width of the transition. The Curie temperature, T_C, was obtained from a fit of the paramagnetic spectral fraction, p, with the model described by Eq. (6), see Fig. 5.

According to the Bean and Rodbell[23] magnetostriction exchange model, the reduced magnetization, σ, and hence the reduced hyperfine field, of a material undergoing a magnetostrictive first-order phase transition is given by

$$\sigma=B_S\left[\frac{3S}{S+1}\frac{\sigma}{\Theta}\left(1+\frac{3}{5}\frac{(2S+1)^4-1}{2(S+1)^3S}\eta\sigma^2\right)\right], \tag{7}$$

where B_S is the Brillouin function for the spin S, $\Theta=T/T_C$ is the reduced temperature for the critical temperature, T_C, and η is the order parameter of the transition. The solution of Eq. (7) for given values of S, Θ, and η, is easily obtained by recursive evaluation with $\sigma_0=0.9$ and $\sigma_{n+1}=f[\sigma_n]$, where $f[\ ]$ stands for the right-hand side of Eq. (7). As few as ca. 90 recursion steps yield an excellent approximation for all reduced temperatures. This recursive evaluation yields the highest of the two values for $\sigma(T)$ that are possible[23,24] between the Curie temperature and the limiting temperature of the first-order phase transition; and the calculated $\sigma(T)$ exhibits a discontinuity at the limiting temperature. The limiting temperature, T_L, above which the system is no longer found in the ferromagnetic state, has a value that increases with η, and is somewhat larger than T_C, for the case $\eta>1$. When $\eta<1$, $T_L=T_C$ and the transition is not a first-order transition.

The parameters resulting from the fit, see Fig. 5, of the measured hyperfine fields with the Bean and Rodbell model are summarized in Table IV. In these fits, T_C values obtained as described above were used. A spin of $S=2$ was estimated from the saturation moments[21,24] and constrained in the fits. As expected[23] for a first-order phase transition, the η_F values that correspond to the ferromagnetic to paramagnetic phase transition are above one. Further, a decrease in η_F with increasing x is observed. This indicates that the critical region T_L-T_C narrows as x increases. Because a larger η_F parameter

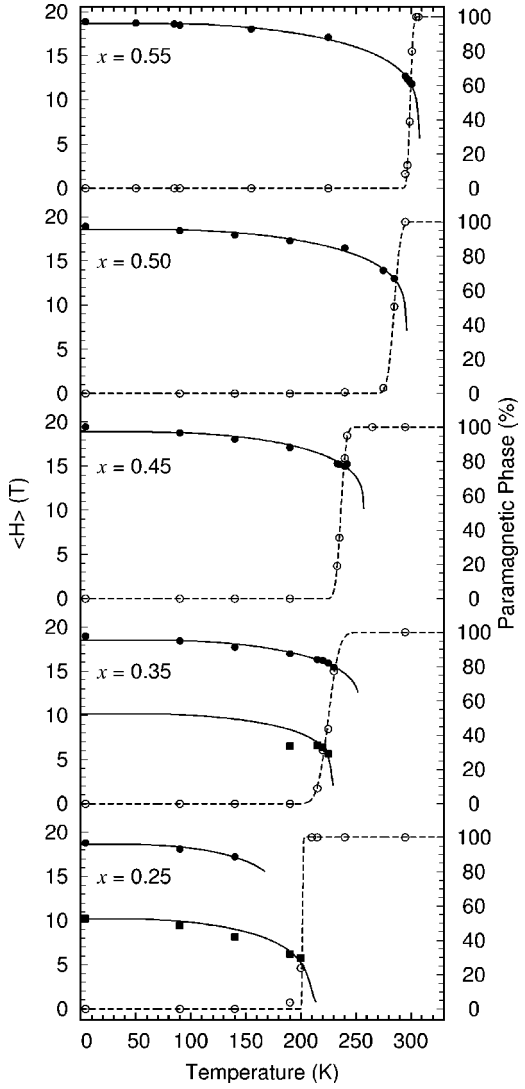

FIG. 5. The average hyperfine field as a function of temperature, solid symblos and the left scale. The percent area of the paramagnetic phase, open circles and the right scale. The hyperfine field of the ferromagnetic phase, solid circles, has been fit with the Bean and Rodbell model (Ref. 23), full line. The percent area of the paramagnetic phase has been fit with Eq. (6), dashed line. The average hyperfine field of the antiferromagnetic phase, closed squares for $x=0.25$ and 0.35, has been fit with the Bean and Rodbell model (Ref. 23), full line.

indicates a more pronounced first-order character for the transition it is not surprising that the magnetocaloric refrigerant capacity is observed to increase, with increasing η_F and decreasing x.[11] Further, it is interesting to note that, even though a microscopic parameter, i.e., the hyperfine field experienced by the iron-57 nuclei, is obtained by Mössbauer spectroscopy in the absence of any applied magnetic field, its temperature dependence leads to magnetic transition parameters that completely agree with those obtained from the macroscopic magnetization measurements, η_F^M,[21,24] obtained in the presence of an applied field.

The Bean and Rodbell[23] model was also applied to the antiferromagnetic to ferromagnetic phase transition, although this transition may not be first order, as indicated by the value of η_{AF} that is close to 1.

TABLE IV. The phase transition parameters for $FeMnP_{1-x}As_x$.

x	T_C, K	w, K	η_F	η_F^{Ma}	$\langle H\rangle$ (0), T	η_{AF}
0.55	299	2.1	1.43	1.75	18.7	
0.50	285	4.7	1.57	1.62	18.6	
0.45	236	3.8	2.0	1.90	18.9	
0.35	225	7.9	2.3	2.43	18.6	1.2[b]
0.25	155[c]/202[d]	2.2	2.6		18.6	0.8[b]

[a]Determined from magnetization measurements (Refs. 21 and 24).
[b]This value was obtained by fixing 10.2 T as the average hyperfine field at 0 K.
[c]This critical temperature for the ferromagnetic phase was estimated and fixed.
[d]The critical temperature, ±10 K, for the antiferromagnetic phase.

VI. THE ANTIFERROMAGNETIC STRUCTURE

The antiferromagnetic structure of the $FeMnP_{1-x}As_x$ compounds, with $x<0.33$, has been reported to be incommensurate.[13,14] For $x=0.2$, the structure is accidentally commensurate and a magnetic model that takes into account the two nearest iron and the six nearest manganese neighbors for each iron has been reported.[14]

The magnetic structures of $FeMnP_{0.75}As_{0.25}$ and $FeMnP_{0.65}As_{0.35}$ are incommensurate and a different approach must be used. The iron and manganese are located in layers perpendicular to the c-axis and, within the iron layer, the iron atoms are grouped in triangles of near neighbors. The iron magnetic moment is known to align in the c-direction. The manganese moments are located in the ac plane and the propagation vector of their helical configuration is perpendicular to this plane.[13] It can then be supposed, to a first approximation, that the moments of the three iron atoms within a triangle are parallel and have the same magnitude. It follows that the hyperfine field experienced by an iron nucleus can be expressed simply as the sum of a constant field, $H_{Fe}=C_1\mu_{Fe}$, a contribution that results from the magnetic field of a particular iron atom and of its two nearest neighbors, and a modulated field, $H_{Mn}=C_2\mu_{Mn}\sin(\theta)$, that results from the six manganese near neighbors, that participate in the incommensurate magnetic structure. This model, described by Eq. (5) and illustrated in Fig. 6, yields excellent fits over the entire compositional and temperature range in which the antiferromagnetic phase has been observed. It should be noted that fits in which the integration of Eq. (5) was conducted over $0\leqslant\theta\leqslant 2\pi$, i.e., in which H_{Fe} and H_{Mn} must be subtracted for the region $\pi\leqslant\theta\leqslant 2\pi$, do not yield satisfactory fits. This is an indication that the direction of the iron moments is always parallel to the projection of the manganese moments on the c-axis, as is depicted in Fig. 6.

As can be seen in Table III, $C_2\mu_{Mn}$ is slightly smaller at 4.2 K than at 90 K. This is an indication that this model does not exactly reflect reality. It is probable that, depending on

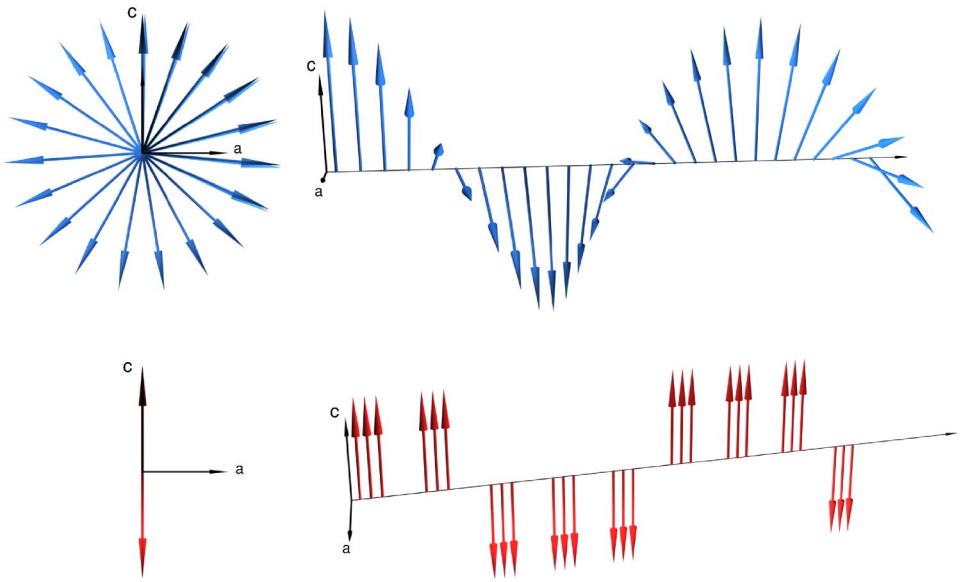

FIG. 6. (Color online) Schematic view of the iron magnetic moments along the *c*-axis, at the bottom, and the manganese magnetic moments, at the top. The left figures show the projection of the moments on the *ac* plane. In the right figures, the propagation direction of the helical manganese moments, towards the right, is perpendicular to the *ac* plane. For clarity the origin of the vector denoting the moment has been projected on the propagation direction, and the triangles of iron near neighbors hence appear as oscillating triplets of moments.

the temperature, the magnetic incommensurability differs and results in varying relative values of the $C_1\mu_{\mathrm{Fe}}$ and $C_2\mu_{\mathrm{Mn}}$ constants. The use of the Bean and Rodbell model[23] to fit $\langle H_{\mathrm{AF}}\rangle$ yields $\eta_{\mathrm{AF}}\sim 0.8$ for $FeMnP_{0.75}As_{0.25}$, a value which is less than 1 and indicates that the antiferromagnetic to paramagnetic phase transition is probably not first order. In the case of $FeMnP_{0.65}As_{0.35}$ the η_{AF} value of 1.2 is probably not reliable, and the proximity of the magnetic triple point combined with the likely inhomogeneities in the sample prevents definite conclusions based on the Mössbauer spectral analysis. The $C_1\mu_{\mathrm{Fe}}$ and $C_2\mu_{\mathrm{Mn}}$ values obtained for $FeMnP_{0.75}As_{0.25}$ can be compared to the values obtained[14] for $FeMnP_{0.8}As_{0.2}$. The reported constant, $a+2b$,[14] related to the iron moments is 5.2 T/μ_B at 80 K and for an iron moment, μ_{Fe}, of $1\mu_B$, is in good agreement with the value of $C_1\mu_{\mathrm{Fe}}=5.8$ T obtained herein at 90 K. The combination of the constants related to the manganese moments, $2c_1+c_2 \simeq 4.5\ \mathrm{T}/\mu_B$,[14] compared with the value of $C_2\mu_{\mathrm{Mn}}=7.2$ T obtained herein at 90 K indicates that the effective moment of the manganese, μ_{Mn}, of ca. $1.6\mu_B$, as experienced by the iron, is substantially smaller than the reported value[13] of $2.4\mu_B$. This difference may result from an underestimation of the manganese moment because in calculating the moment it is assumed that the manganese moments that contribute to the hyperfine field can be summed in a scalar way, whereas the contributing fields from the different manganese neighbors add as vectors that are not parallel. Finally, the coexistence of the antiferromagnetic and ferromagnetic phases is observed between 4.2 and 140 K in $FeMnP_{0.75}As_{0.25}$, as is shown in the phase diagram in Fig. 4. This coexistence can be ascribed to slight inhomogeneities in the sample composition, and are in agreement with the existence of a magnetoelastic ferromagnetic to antiferromagnetic transition.[14,25] The antiferromagnetic phase is however observed over a much larger temperature range than previously reported.

VII. CONCLUSIONS

The Mössbauer spectral analysis of the magnetocaloric compounds $FeMnP_{1-x}As_x$ with $x=0.25$, 0.35, 0.45, 0.50, and 0.55 yields ordering parameters, η_{F}, for the temperature induced ferromagnetic to paramagnetic first-order phase transition in agreement with the parameters obtained from magnetization measurements.[21,24] The observed increase in η_{F} upon decrease of x is an indication of an enhancement of the first-order character of the temperature induced ferromagnetic to paramagnetic transition. This enhancement is probably responsible for the increase in magnetocaloric cooling power with decreasing x.[11]

The phase diagram constructed from the Mössbauer spectral results is in excellent agreement with a previous phase diagram constructed from neutron diffraction measurements,[13] with the exception that herein critical temperatures higher by about 10 K are observed for the ferromagnetic to paramagnetic phase transition for the compounds with $x=0.50$ and 0.55. This discrepancy probably originates from different sample preparations. The samples used for the neutron diffraction measurements[13] were prepared from mixtures of MnFeP and MnFeAs by heating the powder mixtures a short time at 950 °C followed by heating at 750 °C for 2 days. The present samples were prepared from mixtures of Fe_2P, $FeAs_2$, Mn, and P which were first ball milled, then heated for 5 days at 1000 °C and then for 5 days at 750 °C.[3] Although x-ray diffraction showed that the same phase had formed in both cases, the site occupations may be somewhat different and, more specifically, the

iron and manganese antisite disorder, evidenced by the presence of iron on the pyramidal site, may be different in the two sets of samples. The observed difference in critical temperature is of pratical importance because the critical temperature is an important parameter in obtaining a maximal magnetocaloric cooling power near the desired operating temperature in future magnetic refrigeration devices. At this time the precise origin of the higher critical temperature of the compounds used herein cannot be definitely identified, but it would seem that the ball milling preparation[3] yields compounds with a higher critical temperature. Only a simultaneous study of the two sets of samples by x-ray and neutron diffraction and Mössbauer spectroscopy could identify the origin of the differences in the critical magnetic temperatures.

Finally, in addition to the binomial distribution model used for all compounds studied herein, a fitting model, that extends the usual method for fitting incommensurate magnetic structures, is applied to the antiferromagnetic phase observed in $FeMnP_{1-x}As_x$ with $x=0.25$ and 0.35. This model takes into account the influence of both the oscillating iron magnetic sublattice and the helical manganese sublattice, and yields excellent fits over the complete temperature range in which the antiferromagnetic phase is observed.

[1] V. K. Pecharsky and K. A. Gschneidner, Phys. Rev. Lett. **78**, 4494 (1997).

[2] V. Provenzano, A. J. Shapiro, and R. D. Shull, Nature (London) **429**, 853 (2004).

[3] O. Tegus, E. Brück, K. H. J. Buschow, and F. R. de Boer, Nature (London) **415**, 150 (2002).

[4] J. Glanz, Science **279**, 2045 (1998).

[5] P. Debye, Science **81**, 1154 (1926).

[6] W. F. Giauque, J. Am. Chem. Soc. **49**, 1864 (1927).

[7] W. F. Giauque and D. P. MacDougal, Phys. Rev. **43**, 768 (1933).

[8] G. V. Brown, J. Appl. Phys. **47**, 3673 (1976).

[9] A. M. Tishin, in *Handbook of Magnetic Materials*, edited by K. H. J. Buschow (North-Holland, Amsterdam, 1999), Vol. 12, pp. 395–524.

[10] C. Zimm, Adv. Cryog. Eng. **43**, 69 (1998).

[11] O. Tegus, E. Brück, L. Zhang, W. Dagula, K. H. J. Buschow, and F. R. de Boer, Physica B **319**, 174 (2002).

[12] O. Beckman and L. Lundgren, in *Handbook of Magnetic Materials*, edited by K. H. J. Buschow (North-Holland, Amsterdam, 1991), Vol. 6, pp. 181–287.

[13] M. Bacmann, J. L. Soubeyroux, R. Barrett, D. Fruchart, R. Zach, S. Niziol, and R. Fruchart, J. Magn. Magn. Mater. **134**, 59 (1994).

[14] B. Malaman, G. Le Caër, P. Delcroix, D. Fruchart, M. Bacmann, and R. Fruchart, J. Phys.: Condens. Matter **8**, 8653 (1996).

[15] R. Chandra, S. Bjarman, T. Ericsson, L. Häggström, C. Wilkinson, R. Wäppling, Y. Andersson, and S. Rundqvist, J. Solid State Chem. **34**, 389 (1980).

[16] P. Jernberg, A. A. Youssif, L. Häggström, and Y. Andersson, J. Solid State Chem. **53**, 313 (1984).

[17] G. Le Caër and S. M. Dubiel, J. Magn. Magn. Mater. **92**, 251 (1990).

[18] R. H. Herber, in *Chemical Mössbauer Spectroscopy*, edited by R. H. Herber (Plenum, New York, 1984), pp. 199–216.

[19] F. Grandjean, O. Isnard, and G. J. Long, Phys. Rev. B **65**, 064429 (2002).

[20] R. Zach, M. Guillot, and R. Fruchart, J. Magn. Magn. Mater. **89**, 221 (1990).

[21] O. Tegus, G. X. Lin, W. Dagula, B. Fuquan, L. Zhang, E. Brück, F. R. de Boer, and K. H. J. Buschow, in Proceeding of the JEMS 04, Dresden, 2004, J. Magn. Magn. Mater. (to be published).

[22] R. Fruchart, Ann. Chim. (Paris) **7**, 563 (1982).

[23] C. P. Bean and D. S. Rodbell, Phys. Rev. **126**, 104 (1962).

[24] R. Zach, M. Guillot, and J. Tobola, J. Appl. Phys. **83**, 7237 (1998).

[25] R. Zach, M. Bacmann, D. Fruchart, P. Wolfers, R. Fruchart, M. Guillot, S. Kaprzyk, S. Niziol, and J. Tobola, J. Alloys Compd. **262-263**, 508 (1997).